

**Synthesis of Morphine Loaded Hydroxyapatite Nanoparticles (HAPs) and
Determination of Genotoxic Effect for Using Pain Management**

Abstract

Morphine is used as a standard analgesic for intensive pain relief. It relieves acute and chronic pain by acting directly on the central nervous system and to treat myocardial infarction and shortness of breath. However, the use of morphine for the alleviation of chronic pain is controversial because of its adverse side effects. The overall success of this medicine in chronic therapy is due to the long-term activity of the drug at a reasonable concentration. Nanoparticle-based carriers have emerged as a new class of drug delivery systems that can overcome traditional drug side-effect limitations by reducing toxicity to a minimum. In this study, a morphine-loaded HAPs drug delivery system was investigated. Fourier Transform Infrared Spectroscopy (FTIR) analysis was used to characterize typical functional groups found in the chemical composition of Hydroxyapatite Nanoparticles (HAPs) and morphine loaded HAPs (HAP+M). Scanning electron microscopy (SEM) and Transmission electron microscope (TEM) analyses were performed to examine the size, morphology, and porosity of morphine loaded HAPs. The effects of pH on release of morphine-loaded HAPs was determined. In addition, it was investigated whether the morphine loaded HAP cell produced oxidative stress and genotoxic effect on DNA. Findings presented in this paper suggested that morphine-loaded HAPs have a promising future as a nanocarrier for pain treatment.

ABBREVIATIONS

COMET	: Single-cell Gel Electrophoresis
FTIR	:Fourier Transform Infrared Spectroscopy
HA	:Hydroxyapatite
HAP+M	:Morphine loaded Hydroxyapatite Nanoparticles
HAPs	:Hydroxyapatite Nanoparticles
HPLC	:High performance liquid chromatography
IASP	:International Association for the Study of Pain
SEM	:Scanning electron microscopy
TEM	:Transmission electron microscope
USP	:United States Pharmacopeia

33 WHO :World Health Organization

34 TAS :Total antioxidant status

35 TOS :Total oxidant status

36 OSI :The oxidative stress index

37

38

39 **Keywords:** Morphine, HAPs, delivery system, pain therapy.

40

41

42 1. INTRODUCTION

43

44 International Association for the Study of Pain (IASP) defines pain as "an unpleasant sensory
45 and emotional experience linked to or associated with actual or potential tissue damage".
46 Depending on the neuropsychological bases and duration of neuropathic, nociceptive,
47 psychogenic, imaginary, acute and chronic, several different pain subtypes can be described
48 [1]. Many people in the world suffer from chronic pain [2]. It is one of the most common
49 reasons for individuals seeking medical treatment. If the chronic pain is not treated, either life
50 quality may decrease or some dysfunctions such as physical and social may arise.

51

52 Accomplish pain management provides adequate analgesia without extreme side
53 effects. The current pain management method of the World Health Organization (WHO)
54 begins with non-opioid drugs, progresses with weak opioids and results in strong opioids [3].
55 The WHO also suggests adjuvant treatment with antidepressant drugs to help decrease anxiety
56 associated with chronic pain. Pain management can be complicated by the dependence on the
57 drugs used and drug side effects. Many factors can influence the drug trend, including genetic
58 diversity, which can further complicate the management of these factors [4].Morphine is a
59 powerful pain reliever and is used to treat severe pain such as surgery, serious injury, cancer-
60 related pain, or heart attack. It is also used for other chronic pain types where weaker
61 painkillers are no longer effective [4]. Morphine is marketed in the form of tablets, capsules,
62 granules, injectable, and suppositories and can only be used by prescription. It is used as a
63 standard analgesic for intensive pain treatment. It is used directly to relieve acute and chronic
64 pain by acting on the central nervous system. It works by preventing the pain signals moving
65 along the nerve from passing to the brain [5].

66

67 However, the use of morphine for the alleviation of chronic pain is controversial
68 because of the adverse side effects such as addiction, respiratory depression, gastrointestinal
69 effects, and urological effects. The most common side effects of morphine are constipation,
70 feeling sick and insomnia. The use of morphine for the treatment of chronic pain can only be
71 confirmed in patients who do not respond to other treatments. Because the long-term effects
72 of overdose and continuous use of morphine can affect almost all organ systems of the body
73 [5].

74
75 Over the past several decades, nanotechnology has emerged with momentum as a
76 promising new solution to a range of previously unsolvable scientific and technological
77 issues. Nanoparticles offer a massive range of properties and characteristics that can be finely
78 tuned for many applications, from electronics to medicine. More recently, an exploration into
79 their uses in the field of targeted drug delivery has gained popularity with many successes and
80 advancements resulting [6,7,8]. Even with these successes, there has been a delay in the
81 transfer of nanotechnology to the field of pain management. Nanoparticles are available in
82 sizes that are well within the range of typical synaptic gaps through which neurons
83 communicate, and their size also lends them towards possible passage through the blood-brain
84 barrier, a system of tight gap junctions which prevent the passage of large, ionized molecules
85 from entering the central nervous system [9,10]. These size advantages, coupled with the ease
86 of surface modifications and highly tunable characteristics, suggest that the future of pain
87 management lies within the field of nanotechnology.

88
89 Hydroxyapatite (HA) is a bioactive, osteoconductive chemical agent that is neither
90 toxic nor immunogenic [11]. There are several applications of HA such as catalysis, fertilizers
91 and pharmaceutical products, water treatment processes and bone and tooth repair. However,
92 the applications areas are very restricted because of their fragility. Many studies have been
93 carried out to modify HA with polymers since natural bone is a composite consisting
94 essentially of nano-sized pinhole HA crystals (constituting about 65% of bones) [5] and
95 collagen fibers [6]. Extremely thin HA powder has been used to increase the quality of HA
96 [7]. In the literature, a number of methods such as Sol-gel [8,9], reverse microemulsion
97 [10,11], hydrothermal [12], microwave hydrothermal [13], precipitation [14] and solid-state
98 reaction [1] have been reported for HA synthesis. Nano-sized and weak agglomerated HA
99 particles were produced by hydrothermal and microemulsion methods [7]. The most reported
100 method for preparing HA particles is the precipitation method. This process is easy, economic

101 and appropriate for industrial production [7]. Ultrasonication is known to be particularly
102 useful for disrupting aggregates and reducing size and polydispersity of nanoparticles [15].

103
104 HA acts as a prototype for bones and teeth and is also commonly used in medical
105 implants [16]. HA is used in the bone as nano-sized needle-like crystals. HA can be used in a
106 variety of forms including powder, granules, porous grains. It is necessary to characterize the
107 HA powder depending on the desired application. Some parameters such as purity,
108 crystallinity, and morphology can be controlled when the wet synthesis technique is used.
109 Applications of morphologies can differ. For example, although spherical particles are used in
110 thermal spray coating, needle-shaped or rod-shape are used in bone repair composite material
111 [17]. Recently, nano-HA has attracted the attention of researchers thanks to the important role
112 of HA in several biomedical applications. There are a few methods including chemical
113 precipitation, spray drying, sol-gel to synthesize HA. The nanoparticle size of the HA crystal
114 is an average length of 50 nm and is embedded in the collagen matrix in natural bone and
115 teeth. Actually, collagen acts as a template in the collagen-controlled bio-mineralization
116 process [18].

117
118 A long-acting product formulation from the morphine will have the potency of both
119 patient rehabilitation and patient comfort. The overall success of this drug in chronic therapy
120 is due to its long-term activity at a reasonable concentration around the action area. After
121 entering the host, the nanoparticles, which have a reasonable density near the domain,
122 function as a drug reservoir capable of releasing the drug for a long time in the bloodstream.
123 This long-acting drug profile is used as a basis for long-term chronic drug action to the
124 desired effect. For these reasons, there is a need to develop a morphine-loaded nanoparticle
125 drug release system without any cytotoxicity threat. In addition, there is a need to be
126 developed to release the morphine loaded drug slowly and in a controlled manner into the
127 action zone.

128
129 In this study, the first time morphine loaded HAPs (HAP + M) were synthesized and
130 partial characterization was performed. The effect of morphine release of pH was investigated
131 and the genotoxicity of HAP + M was determined by comparing the comet assay and
132 oxidative stress parameters.

133
134 **2. MATERIALS AND METHODS**

135

136 **2.1. Materials**

137 Poppy capsules were obtained from Opium Alkaloid Plant (Turkish Grain Board). The
138 capsules were broken and their seeds are separated. Poppy capsules were dried at room
139 temperature for 15 days in a dark room at room temperature. It was ground to the size of 80
140 mesh grain size before extraction. Morphine Reference Standard was obtained from the
141 United States Pharmacopeia (USP). All chemicals used in all experiments were in analytical
142 quality and in High performance liquid chromatography (HPLC) grades all solvents used for
143 chromatographic purposes. All chemicals were purchased from Sigma Aldrich. 0.45 μm
144 membranes (Millipore, Bedford) were used for the filtration of all solutions.

145

146 **2.2. Extraction of morphine from poppy capsules.**

147 Alkaloids are produced by using natural products or synthetically. Because of the low toxicity
148 of natural products, they are preferred from the pharmaceutical industry. Therefore, the study
149 is done by extracting morphine from poppy capsules. 100 g of dried and the ground sample
150 was weighed into a 2 L of the beaker. 1000 ml of solvent (80 % Methanol + 20 % 0.1 M HCl)
151 was added over the capsules. Morphine was extracted for one day by constant stirring. The
152 mixture was filtered off 500 ml of solvent (80 % Methanol + 20 % 0.1 M HCl) for the second
153 extraction was added on the poppy pulp. The mixture was filtered off. All extracts obtained
154 from three extractions were combined for purification. The combined extract was evaporated
155 under vacuum at 40 °C in a rotary evaporator to 200 ml of a total volume. 200 mL of
156 concentrated aqueous extract was left. Concentrated extract was kept in the refrigerator at the
157 temperature of (0-4 °C) for one day. The extracts were filtered and plant-derived wax,
158 tannins, and oily substances were separated and thrown. A small amount of diatomaceous
159 earth was added to remove the impurities in the concentrated extract solution to obtain a
160 clearer extract, and the mixture was stirred at 50 °C for half an hour. The mixture was filtered
161 through white band strainer paper. A more transparent extract was obtained.

162

163 The concentrated extract was extracted 3 times with petroleum ether to remove the
164 vegetative oily substances in the concentrated extract. In each extraction, the aqueous
165 concentrate extract and the petroleum ether were stirred for 15 minutes. It was left for 15
166 minutes and the phases were allowed to separate. The morphine-free petroleum ether phase
167 was discarded. Active carbon is used to remove undesirable compounds that can cause color,
168 quality, and property changes in liquids due to its enabling feature of final product in the

169 pharmaceutical industry to be uncolored and purified. For this, a small amount of activated
170 carbon was added to the extract, stirred at 50 °C for half an hour and filtered. This process
171 was repeated three times. Finally, the concentrated extract was evaporated to a saturation
172 concentration in a rotary evaporator. The amount of morphine in the concentrated extract was
173 determined by HPLC analysis [19].

174

175 **2.3. Preparation of morphine loaded HAPs (HAPs) with precipitation method using** 176 **ammonium phosphate and calcium nitrate solutions**

177 HAPs were prepared using an aqueous precipitation technique. The molar concentration of
178 calcium nitrate tetrahydrate and diammonium hydrogen orthophosphate was adjusted to have
179 a theoretical value of the Ca/P ratio: 1.667. 0.156 M stock solution of diammonium hydrogen
180 orthophosphate in demineralized water and 0.400 M stock solution of calcium nitrate
181 tetrahydrate in absolute ethanol were used. These solutions were continuously mixed at a
182 temperature of 70 °C for 4 h on the magnetic stirrer. 100 mL of diammonium hydrogen
183 orthophosphate solution was added to the beaker to synthesize morphine-loaded HAPs. The
184 solution was heated to 70 °C. 50 mL of concentrated morphine solution was added over its.
185 100 mL of the calcium nitrate solution was added dropwise to this mixture for an hour. The
186 mixture was stirred at 70 °C for 4 hours. The precipitated white colored nanoparticles were
187 filtered using white band filter paper and washed three times with double distilled water and
188 finally with ethanol. Nanoparticles powder were dried in an oven at 105 °C for 4 hours until it
189 gets dry.

190

191 **2.4. Characterization Analysis of HAPs**

192 **2.4.1. Determination of Morphine Contents by HPLC Analysis**

193 In our study, HPLC analyzes were used to determine that morphine content was loaded into
194 HAP. Therefore, % purity control was not carried out in the extraction steps.
195 Chromatographic analyzes were performed on an Agilent brand 1260 model HPLC
196 instrument (Agilent, USA). The system includes a quaternary gradient pump, vacuum
197 degasser, column thermostat, automatic sampler, and (UV/VIS) detector. The Chem Station
198 software was used to collect and evaluate data. Chromatographic separation was performed
199 with an ACE C18 column (5 µm, 150 mm * 4.6 mm I. D.). Mobile phase A was a solution of
200 5 % acetonitrile and mobile phase B was a mixture of acetonitrile: glacial acetic acid:
201 trimethylamine in the ratio of (97.9: 2: 0.1, v / v). The flow rate of the mobile phase was 1
202 mL/min; Column thermostat temperature was maintained at 30 °C; Injection volume was 50

203 μl ; Detection was carried out at 284 nm; Working time: 30 minutes. Elution was performed
204 with the gradient: 0 min 10% solvent B; 0–5 min from 10 to 15% solvent B; 5–10 min from
205 15 to 20% solvent B; 10–20 min from 20 to 35% solvent B; 20–30 min from 35 to 10%
206 solvent B [20].

207

208 To analyze the amount of morphine in the morphine-loaded nanoparticle, 200 mg of
209 nanoparticle was weighed into a 100 mL beaker. 20 ml of 0.1 molar HCl was added and
210 dissolved in the ultrasonic bath. Transferred to a 50 ml balloon, the volume was completely
211 deionized water. The amount of morphine in the resulting solution was analyzed by HPLC.

212

213 **2.4.2. FTIR analysis**

214 FTIR analysis was carried out to determine the various phosphate and carbonate functional
215 groups in the synthesized HAPs. HAPs dried at 105 °C was analyzed for FTIR analysis.
216 Spectrum Two model of Perkin Elmer brand FTIR Spectrometer was used in FTIR analysis.

217

218 **2.4.3. Scanning electron microscopy (SEM) analysis**

219 SEM analysis was performed to determine the morphological and grain sizes of the
220 synthesized nanoparticles. Phenom brand ProX model SEM device was used in the analysis.

221

222 **2.4.4. Transmission electron microscope (TEM) analysis**

223 TEM analysis was performed to clarify the size, shape, morphology and internal structure of
224 the nanoparticles. JEOL JEM-2100 transmission electron microscope (UHR) device was used
225 in the analysis.

226

227 **2.5. The effect of pH on morphine-loaded drug release**

228 A NaCl / HCl solution with a pH of 1.2 (stomach pH) and 7.4 (intestinal pH) were prepared.
229 The release tests were carried out at a temperature of 37 ± 0.5 °C (human body temperature)
230 in a horizontal shaking kiln at 100 rpm. 200 mg powder of morphine loaded HAPs was
231 weighed to a beaker of 100 mL and added 20 mL of the PBS solution. The morphine amount
232 in the prepared medium is 14.2 ppm. Erlenmeyer was covered with aluminum foil and was
233 placed in a shaker oven 100 rpm at 37 °C. 2 mL of samples was taken at every five hours. The
234 samples were analyzed by HPLC after filtration through an injector filter [21]. Measurements
235 were continued until the drug release was fixed.

236

237 **2.6. Comet assay**

238 The blood samples was collected from a healthy and non-smoking young donor at the age of
239 28. Leukocytes were isolated over Histopaque 1083 gradients by centrifugation at 2100 rpm
240 for 20 min at 15 °C. The comet assay was performed under alkaline conditions according to
241 Singh et al. (1988) with some modifications. Isolated human leukocytes (100 µL) were
242 incubated with 100 µL different concentrations of HA and HA+M (5, 10 and 25 mg/mL) for 1
243 h at 37°C [22]. a Positive (30 mM H₂O₂) and a solvent control (1XPBS) were also included.
244 Following the incubation, leucocytes were at 1600 rpm for 10 min at 25 °C. While
245 supernatant was used for TAS and TOS determination, the pellet was used for Comet assay.
246 The Comet assay protocol was done according to Avuloglu-Yilmaz et al. (2017) [23]. The
247 analysis of comet scores was calculated as described by the Cigerci et al. (2015) [24].

248

249 **2.7. Measurement of total oxidant status and oxidative stress index**

250 TOS and TAS were determined spectrophotometrically using Rel Assay Diagnostic kit
251 RL0024 and RL0017 reading at 530 nm and 660 nm respectively by Elisa Thermo
252 Scientificific. (Chiaz marka ve ülke ismi) TAS and TOS value was calculated according to
253 the following formula; TOS: $(\Delta\text{AbsSample}) / (\Delta\text{absStandard}) \times \text{Conc. of standard}$ TAS:
254 $((\Delta\text{Abs H}_2\text{O}) - (\Delta\text{Abs Sample})) / ((\Delta\text{AbsH}_2\text{O}) - (\Delta\text{Abs Standart}))$. The oxidative stress index
255 (OSI) of samples were determined with the ratio of TOS to TAS.

256

257 **2.8. Statistical analysis**

258 The scores were presented as means \pm standard deviation. The levels of significance in
259 different treatment groups were analyzed Duncan multiple range tests by using SPSS 23.0
260 version for Windows software. $P < 0.05$ was set as statistical significance.

261

262 **3. RESULTS AND DISCUSSION**

263

264 **3.1 Morphine Contents of Morphine Loaded Nanoparticles by HPLC**

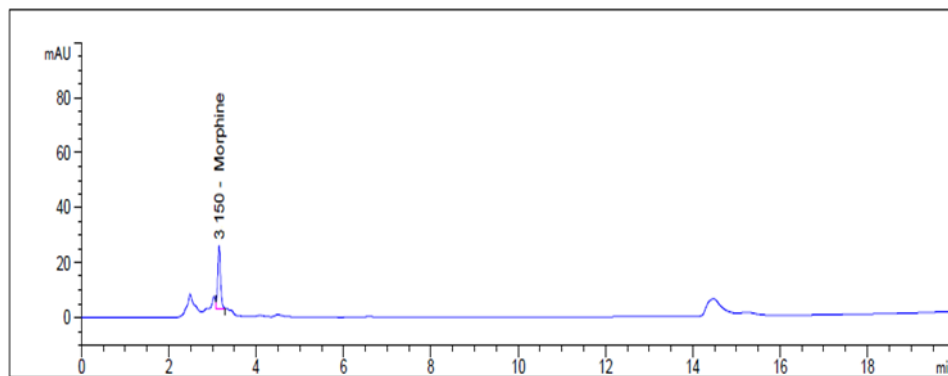
265 As a result of HPLC analysis, the content of morphine in the poppy capsules was determined
266 as 281,6 ppm and the content of morphine in the nanoparticle was determined as 14.2 ppm
267 (Table 1). The HPLC chromatogram of HAPs was shown in Figure 1. Extra peaks except
268 morphine which are seen in Fig. 1 is due to solvent. It was determined that morphine was
269 loaded into HAP as pure.

270

271 **Table 1 The amount of morphine**

Extraction stages	The amount of morphine (ppm)
First extraction	281,6
Second extraction	490,5
Third extraction	2872,8
Morphine in the nanoparticle	14,2

272

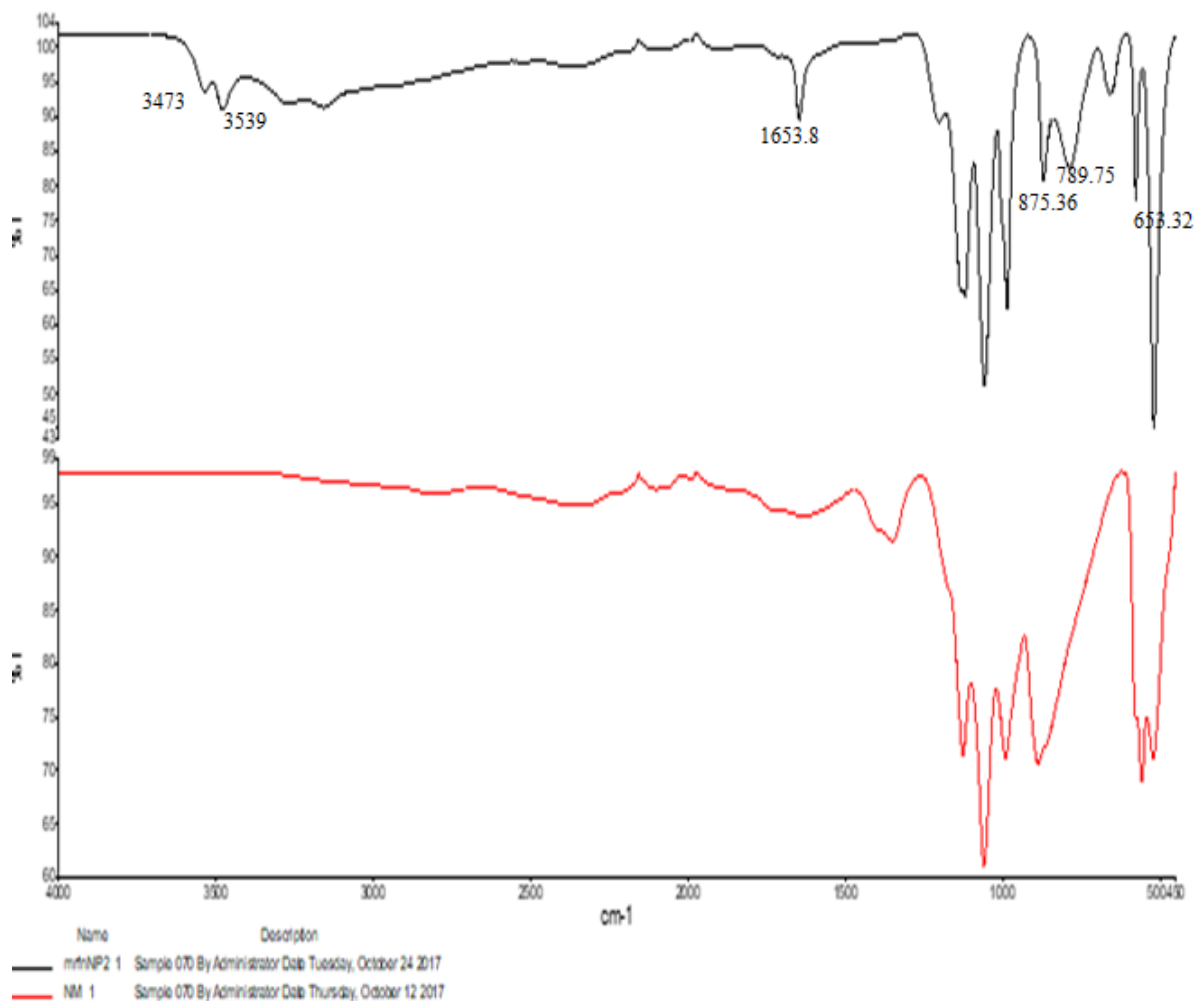


273

274 **Figure 1 HPLC chromatogram of morphine loaded HAPs.**

275

276 Functional groups associated with HA were identified by FTIR spectroscopy. The FTIR
 277 spectra of morphine loaded HAPs and HAPs were shown in Figure. According to Figure 2,
 278 the absorption bands at 1346 cm^{-1} and 886 cm^{-1} show the presence of $(\text{CO}_3)^{2-}$ in HA structure.
 279 The absorption bands at 1060 cm^{-1} detected in the spectra are attributed $(\text{PO}_4)^{3-}$ groups. HA
 280 has been revealed by the absence of a large peak at 3550 cm^{-1} attributed to the crystallization
 281 water and the water molecules trapped in the apatite unit cell. Although nonstoichiometric HA
 282 can contain some water molecules, stoichiometric HA cannot contain water molecules
 283 generally in its unit cell. Absorption bands at 3571 cm^{-1} and 629 cm^{-1} show the presence of
 284 hydroxyl ion in the apatite lattice. Absorption bands observed at 1124 , 1060 , 993 , 886 and
 285 562 cm^{-1} show $(\text{PO}_4)^{3-}$ groups [25,26]. Misra et al (2011) determined morphine absorption
 286 bands in FTIR [27]. Similarly, in this study; FTIR spectrum of morphine-loaded HAPs was
 287 observed to contain different peaks (653.32 , 789.75 , 875.36 , 1653.8 , 3473 , 3539 cm^{-1}) due to
 288 the morphine when compared to the spectrum of HAP (Fig 2).



289

290

291 **Figure 2 FTIR spectrum of morphine loaded HA and unloaded HAPs, respectively.**

292

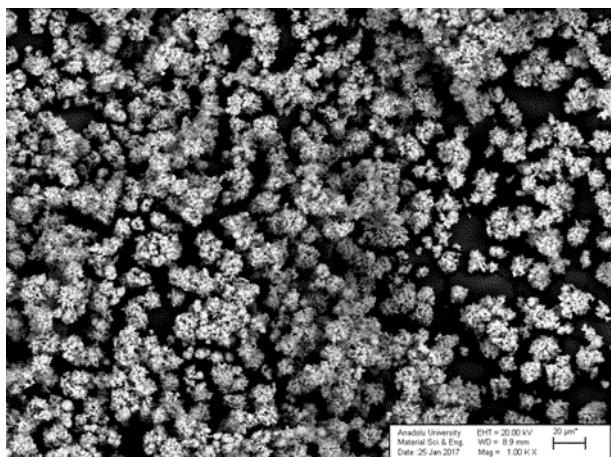
293 **3.3. Scanning electron microscopy**

294 Studies show that the morphology (Irregular, sphere, rod, needle, platelet, tube, fiber,
 295 filament, wire, whisker, strip, platelet, flower) and magnitude of HAP (3 nm sp 1000 μm)
 296 may vary depending on the synthesis method used [28,29,30].

297

298 The morphologies of the synthesized powders were observed by SEM and it was shown in
 299 Fig. 3. The samples are mostly composed of fine-grained and homogeneous particles. The
 300 produced spherical particles can be stacked at high levels, most of the particles are submicron
 301 and nano-sized, as shown in Fig. 3. Since HA provides a porous surface structure, the
 302 predominant size of the particles is in the range of 90-150 nm.

303



304

305 **Figure 3 SEM image of morphine loaded HAPs**

306

307 The crystal structures of apatite have been studied in details [31]. The HAP lattice consists of
308 Ca^{2+} , PO_4^{3-} and OH^- ions distributed over two mirror symmetric halves of the unit cell [32].

309 As a result of point analysis, Ca and P ions were detected in empty HAP (Fig 4). These ions in
310 the structure of hydroxyapatite [$\text{Ca}_5(\text{PO}_4)_3(\text{OH})$] are proof that the desired HAP is formed as
311 shown Fig 5.. The structure of morphine ($\text{C}_{17}\text{H}_{19}\text{NO}_3$) contains nitrogen ions (fig 5). As a
312 result of the SEM point analysis, the determination of the nitrogen with charged particles has
313 shown that morphine is loaded with morphine into HAP (fig 4). In this study, SEM point
314 analysis shows that both the empty HAP and the morphine loaded HAP are obtained.

315

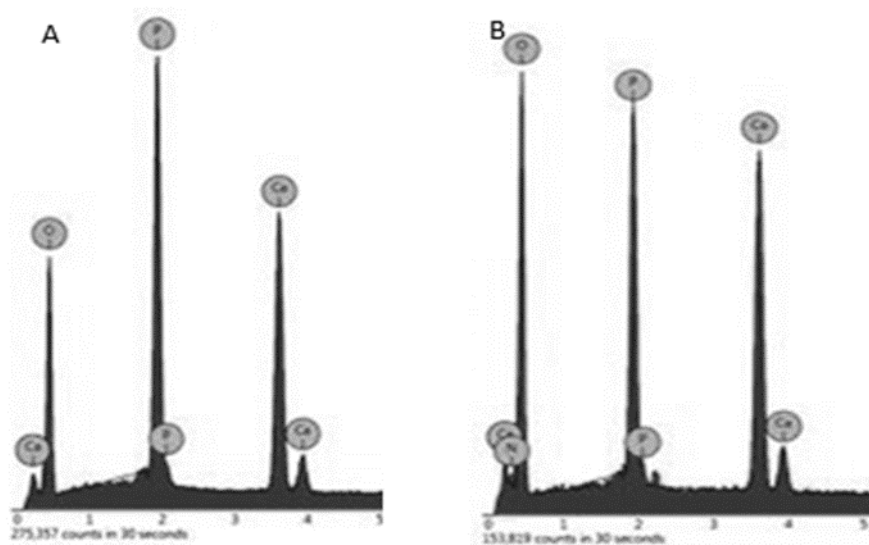
316 There are few articles about the mechanisms of involvement of biomolecules on the surface of
317 HAP particles. Therapeutic agents can interact with the surface of the nanoparticles in two
318 different ways. One is through detachable covalent connections and the other through physical
319 interactions. The amino or hydroxyl groups on the surface of the nanoparticles are effective in
320 covalent binding. Physical interactions such as electrostatic, hydrophobic/hydrophilic and
321 affinity ones can lead to coupling of drug molecules with the surfaces of nanoparticles [33].

322

323 In a single cell unit of HAP, there are 10 PO_4^{3-} groups of a unit cell, two remain inside and
324 eight at the periphery. The positively charged morphine molecules we have obtained are most
325 likely bound by weak electrostatic bonds within the hexagonal structure of the HAP
326 nanoparticles. Binding occurred between the negative charges of the polarized morphine ends
327 and the positively charged phosphate ions in the HAP.

328

329

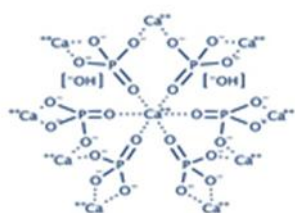


330

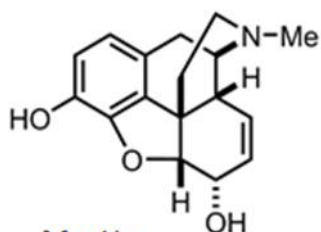
331 A; HAPs B; HAP+M

332 **Figure 4 Point analysis of empty (A) and morphine loaded (B) nanoparticle**

333



Hydroxyapatite



Morphine

334

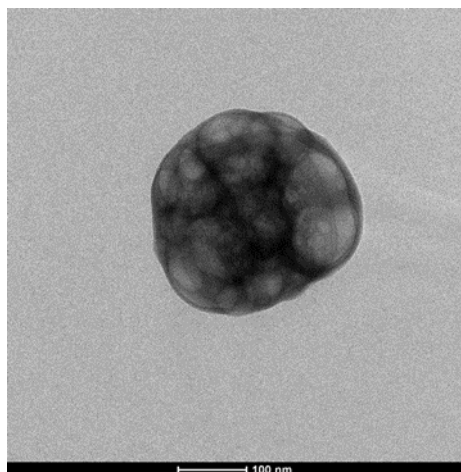
335

336 **Figure 5 Chemical structure of HA and morphine**

337

338 3.4. Transmission electron microscopy

339 Figure 6 shows TEM images of morphine loaded HA nanoparticle samples. The results
 340 demonstrated that the shape of morphine loaded HA nanoparticle samples is a spherical
 341 shape. Nanoparticle sizes were observed to be average 100 nm.



342 **Figure 6 TEM images of morphine loaded HA nanoparticle samples.**

343

344 **3.5. Comet Assay**

345 Since genotoxicity tests of many commonly used drugs are found to be positive, it has
346 become mandatory to screen for mutagenic and carcinogenic potentials of new drugs. It has
347 been reported that morphine causes a significant increase in micronucleus count and DNA
348 damage depending on the dose [34]. Morphine has a genotoxic effect through reactive oxygen
349 species (ROS) causing oxidative stress like other opioids [35,36,37]. In addition, Morfin
350 causes DNA damage by inhibiting oxidative stress enzymes such as Glutathione peroxidase,
351 Glutathione, Superoxide dismutase [38].

352

353 There is clear evidence that drugs can lead to oxidative stress. Oxidation on DNA results in
354 various lesions such as abasic zones and single or double helix fractures.

355

356 There is clear evidence to implicate drug-induced oxidative stress as a mechanism of toxicity.
357 Oxidation of DNA leads to the formation of lesions including oxidized bases, abasic sites, and
358 DNA single- and/or double-strand breaks. One of the reliable techniques for determining
359 oxidative DNA damage is single-cell gel electrophoresis (comet) assay [39]. COMET test is
360 preferred by a number of researchers in toxicity studies due to its precision, speed and
361 economy. In particular, showing DNA damage is a very useful and successful technique.
362 Shafer et al. (1994) observed dose- dependent, significant increases in the frequency of comet
363 tails of fragmented DNA when cells were treated with morphine (5×10^{-9} / 10^{-7} M) [40].
364 According to Even though indirect measurements of oxidative stress level indicates the
365 generation of ROS by HAP, no significant effects associated with ROS mediated cellular

366 damage was evident suggesting the levels of ROS generated is not crossing the threshold level
367 which the system could manage [41].

368
369 In this study, the genotoxic effect of morphine-loaded HAP (HAP+M) was evaluated by
370 measuring the values of both comet and oxidative stress parameters (TAS, TOS and OSI).
371 The effect of HAP and HAP+M on DNA damage is given to Table 2. All tested
372 concentrations increased DNA damage in a dose-dependent manner for HA ($r=-0.891p=0.01$)
373 and for HAP+M ($r=-0.905 p=0.01$). The significant DNA damage was induced after HA
374 except for 5 mg/mL and after HAP+M at 25 mg/mL. While the highest DNA damage was
375 observed the positive control (271.67 ± 4.37), the lowest one observed in the control group
376 (0.33 ± 0.33). 25 mg/L of HAP+M significantly reduced DNA damage compared to HAP.

377

378 **Table 2 Protective effect of HO leaf extract against to H₂O₂**

379

380

Treatment	DNA Damage (Arbitrary Unit \pm SD)*
Control	0.33 ± 0.33^a
30 μ M H ₂ O ₂	271.67 ± 4.37^b
25 mg/L HAP	110.67 ± 2.33^c
10 mg/L HAP	8.33 ± 0.67^d
5 mg/L HAP	1.67 ± 0.33^{ae}
25 mg/L HAP+M	6 ± 0.67^{de}
10 mg/L HAP+M	1 ± 0.58^{ae}
5 mg/L HAP+M	-

381 * Means with the same letter do not differ statistically at the level of 0.05. SD: Standard Deviation

382 HAP; HA nanoparticle, HAP+M; morphine loaded HA nanoparticle

383

384 No significant difference was observed between the 5 mg / mL HAP + M and control group.
385 When the concentration increased, total oxidant capacity increased and total antioxidant
386 capacity decreased. 10 and 25 mg / mL of HAP and 25 mg / mL of HAP + M were found to
387 be statistically significant compared to the control group (Table 3).

388

389 **Table 3. Total oxidant and antioxidant capacity**

	TAS (mmol Trolox Equiv./ L.)	TOS (mM H ₂ O ₂ Equiv. / L.)	OSI
Control	19.14±3.15 ^a	5.54±0.17 ^a	3.54±0.17 ^a
30 µM H ₂ O ₂	5,21±0,25 ^b	19±4,25 ^b	10.54±0.15 ^b
25 mg/ mL HAP	8,12±0,21 ^c	14±1,23 ^c	8.21±0.49 ^c
10 mg/ mL HAP	12±1,71 ^d	10±1,51 ^d	5.95±0.18 ^d
5 mg/ mL HAP	16,57±0,41 ^{a,c}	7,01±1,11 ^{a,c}	4.52±0.6 ^{a,c}
25 mg/mL HAP+M	15,90±1,11 ^{c,d}	8,10±1,11 ^{c,d}	6.04±0.78 ^d
10 mg/mL HAP+M	18,11±1,47 ^{a,c}	5,11±0,47 ^{a,c}	5.4±2.11 ^c
5 mg/mL HAP+M	20,13±1,05 ^a	4,15±0,15 ^a	3.65±0.73 ^a

390

391

392 3.7. The effect of pH on morphine-loaded HAP release

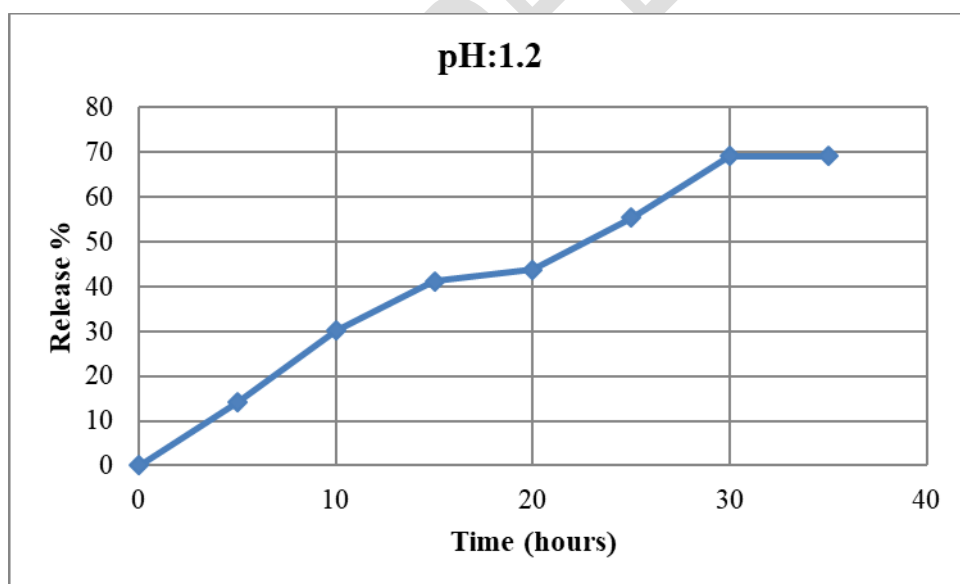
393

394 The graph showing drug release in pH:1.2 as a function of time was given in Figure 7.

395 Morphine-loaded HAPs were found to release a maximum of 69.3 % at the end of 30 hours in

396 pH:1.2.

397



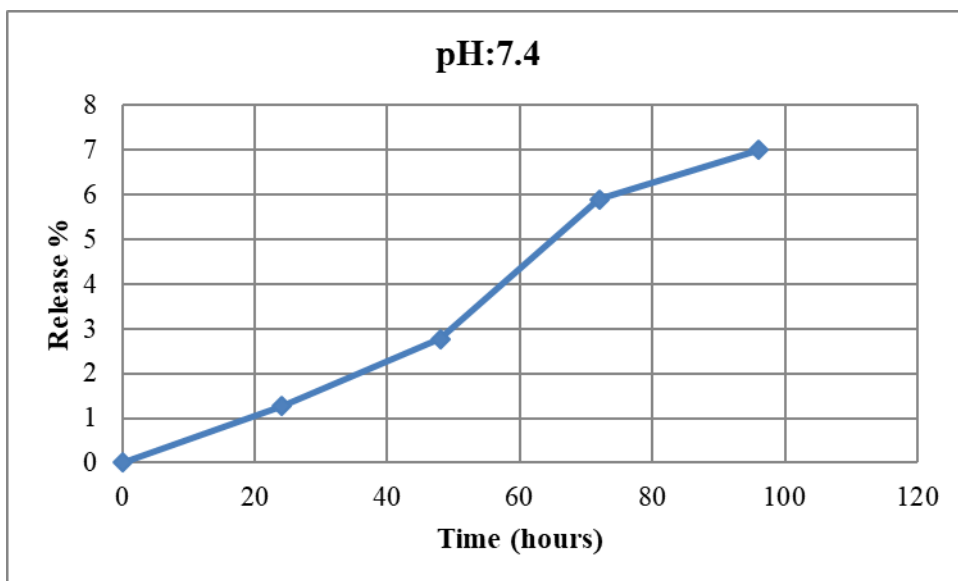
398

399 **Figure 7 The graph showing drug release in pH:1.2.**

400 The graph showing drug release in pH:7.4 as a function of time was given in Figure 8.

401 Morphine-loaded HAPs were found to release a maximum of 7.0 % at the end of 95 hours in

402 the intestinal environment.



403

404

405 **Figure 8 The graph showing drug release in the intestinal environment.**

406

407 Matsumoto et al (2004) reported that release of protein in Ph 4 was higher than Ph 7 .0 at
 408 protein loaded HAP. This is because solubility of HA is greatly affected by the pH. In general,
 409 a more acidic environment causes HA to become more soluble, while a less acidic
 410 environment makes HA less soluble.

411

412 **4. Conclusion**

413

414 The development of morphine-based controlled release formulations for chronic pain
 415 management is an extremely important issue. Other options should be used for drug delivery
 416 aiming at obtaining effective, safe and innovative products. The literature has shown that
 417 binding of morphine to particulate systems not only provides sustained and controlled release
 418 of the drug but also provides a superior or equivalent analgesic profile and reduced side effect
 419 formation from free radicals. HA appears to be an interesting alternative to future studies,
 420 considering the wide range of advantages of nanoparticles and the lack of study of morphine.
 421 Current studies are still not enough to revive the production of new products containing
 422 morphine-loaded nanoparticles in the pharmaceutical industry.

423

424 In this study, it was determined that HAP can be used as a nongenotoxic morphine transport
 425 system. However the drug load of the carrier can be increased and controlled release is

426 achieved with modifications to the HAP molecule. Subsequent studies should be based on
427 release modeling of the morphine charged HAP nanoparticle at in vivo and invitro media.

428

429

430 REFERENCES

431

- 432 1. Bonica JJ. The need of a taxonomy. *Pain*. 1979; 6:247-248.
- 433 2. Furlan AD, Reardon R, Wepler C. Opioids for chronic noncancer pain: a new
434 Canadian practice guideline. *Can Med Assoc J*. 2010; 182:923–30
- 435 3. Hardt J, Jacobsen C, Goldberg J, Nickel R, Buchwald D. Prevalence of chronic pain
436 in a representative sample in the united states. *Pain Med*. 2008; 9:803-812
- 437 4. Kroenke K, Krebs E, Wu J, Bair MJ, Damush T, Chumbler N, et al. Stepped care
438 to optimize pain care effectiveness (scope) trial study design and sample
439 characteristics. *Contemp Clin Trials*. 2014; 34: 270-281
- 440 5. Martin C, De Baerdemaeker A, Poelaert J, Madder A, Hoogenboom R, Ballet S.
441 Controlled-release of opioids for improved pain management. *Materials Today*. 2016;
442 19(9): 491–502
- 443 6. Woodle MC. Sterically stabilized liposome therapeutics. *Adv. Drug Deliv. Rev*. 1995;
444 16(2–3): 249–265
- 445 7. Anselmo AC, Mitragotri S. (2014). Cell-mediated delivery of nanoparticles: Taking
446 advantage of circulatory cells to target nanoparticles. *J. Control. Release*. 2014; 190:
447 531–541.
- 448 8. Rossi F, Ferrari R, Papa S, Moscatelli D, Casalini T, Forloni G, Perale G, and
449 Veglianesi P. Tunable hydrogel-Nanoparticles release system for sustained
450 combination therapies in the spinal cord. *Colloids Surfaces B Biointerfaces*. 2013;
451 108:169–177
- 452 9. Choi YS, Lee MY, David AE, Park YS. Nanoparticles for gene delivery: therapeutic
453 and toxic effects. 2014; *Mol. Cell. Toxicol.* 10 (1): 1–8
- 454 10. Bao G, Mitragotri S and Tong, S. Multifunctional nanoparticles for drug delivery and
455 molecular imaging. *Annu. Rev. Biomed. Eng*. 2013; 15:253–82
- 456
- 457 11. Khaled RM, Hanan HB, Zenab M El-Rashidy. In vitro study of nano-
458 HA/chitosan–gelatin composites for bio-applications. *Journal of Advanced*
459 *Research* . 2014; 5: 201–208

- 460 12. Wang F, Li M, Lu Y. A simple sol-gel technique for preparing HA
461 nanopowders. *Mater. Lett.* 2005; 59:916-919
- 462 13. Kim I, Kumta PN. Sol-gel synthesis and characterization of nanostructured HA
463 powder. *Mater. Sci. Eng. B.* 2004; 111: 232-236
- 464 14. Sun Y, Guo G, Wang Z, Guo H. Synthesis of single-crystal HAP nanorods. *Ceram.*
465 *Int.* 2006; 32: 951-954
- 466 15. Koumoulidis GC, Katsoulidis AP, Ladavos AK, Pomonis PJ, Trapalis CC, Sdoukos
467 AT, Vaimakis TC. Preparation of HA via microemulsion route. *J. Colloid Interface*
468 *Sci.* 2003; 259: 254-260
- 469 16. Yin G, Liu Z, Zhan J, Ding F. and Yuan N. Impacts of the surface charge property
470 on protein adsorption on HA. *Chemical Engineering Journal.* 2002; 87(2): 181– 186.
- 471 17. Kramer E, Podurciel J and Wei M. Control of HA nanoparticle morphology using wet
472 synthesis techniques: Reactant addition rate effects. *Materials Letters.* 2014; 131: 145 –
473 147.
- 474 18. Mostafa AA, Oudadesse H, Mohamed MB, Foad ES, Le Gal Y and Cathelineau G.
475 The convenient approach of nanoHA polymeric matrix composites. *Chemical*
476 *Engineering Journal.* 2009; 153(1): 187 – 192.
- 477 19. Taş CA, Korkusuz F, Timuçin M, Akkaş N. An investigation of the chemical
478 synthesis and high-temperature sintering behaviour of calcium HA and tricalcium
479 phosphate (TCP) bioceramics. *J Mater Sci Mater Med.* 1997; 8:91-6.
- 480 20. Endlová L, Laryšová A, Vrbovský V, Navrátilová Z. Analysis of Alkaloids in Poppy
481 Straw by High-Performance Liquid Chromatography, *IOSR Journal of Engineering.*
482 2015; 05:1-7.
- 483 21. Gün M. Aljinat-Kitosan Nanopartiküllerin Kolşisin Salımında Kullanılmasının
484 Araştırılması, Yüksek Lisans, Kimya Anabilim Dalı Programı Adnan Menderes
485 Üniversitesi Fen Bilimleri Enstitüsü. 2013
- 486 22. Singh NP, McCoy MT, Tice RR, Schneider EL. A simple technique for quantitation
487 of low levels of DNA damage in individual cells. *Exp Cell Res.* 1988; 175:184– 191.
- 488 23. Avuloğlu Y, Yüzbaşıoğlu D. Evaluation of genotoxic effects of 3-methyl-5-(4-
489 carboxycyclohexylmethyl)-tetrahydro-2H-1,3,5-thiadiazine-2-thione on human
490 peripheral lymphocytes. *Pharmaceutical biology.* 2017; 55(1): 1228–1233
- 491 24. Çiğerci IH, Liman R, Özgül E, Konuk M. Genotoxicity of indiumtin oxide by Allium
492 and Comet tests. *Cytotechnology.* 2015; 67:157–163

- 493 25. Feng W, Li MS, Lu YP. and Qi YX, Liu YX. Synthesis and microstructure of HA
494 nanofibers synthesized at 37°C, *Materials Chemistry and Physics*.2006; 95: 145-149
- 495 26. Cengiz B. Hidroksiapatit Nanoparçacıklarının Sentezi, Yüksek Lisans, Kimya
496 Mühendisliği Anabilim Dalı, Fen Bilimleri Enstitüsü. 2007
- 497 27. Misra N, Dwivedi , Pandey AK and Trived S. Vibrational analysis of Two Narcotic
498 Compounds- Codeine and Morphine - A comparative DFT study. *Der Pharma.*
499 *Chemica*.2011; 3(3):427-448
- 500 28. Padmanabhan SK, Balakrishnan A, Chu MC, Lee YJ, Kim TN, Cho SJ. Sol-gel
501 synthesis and characterization of HA nanorods. *Particuology*. 2009;7:466-470.
- 502 29. Shojai MS, Khorasani MT, Khoshdargi ED, Jamshidi A. Synthesis methods for
503 nanosized HA with diverse structures. *Acta Biomater*. 2013; 9:7591-7621
- 504 30. Mobasherpour I, Heshajin MS, Kazemzadeh A, Zakeri M. Synthesis of
505 nanocrystalline HA by using precipitation method. *J Alloys Compd*. 2007; 430:330-
506 333.
- 507 31. Naray SS. The structure of apatite (CaF)Ca₄(PO₄)₃. *Z Kristallogr*. 1930; 75:387-398.
- 508 32. Mondal S, Dorozhkin S, Pal U. Recent progress on fabrication and drug delivery
509 applications of nanostructured HA .*Wiley Interdiscip Rev Nanomed*
510 *Nanobiotechnol*.2018;10(4): doi: 10.1002/wnan.1504.
- 511 33. Kong L, Mu Z, Yu Y, Zhang L, Hu J. Polyethyleneimine- stabilized HAPs modified
512 with hyaluronic acid for targeted drug delivery. *RSC Adv* 2016, 6:101790-101799.
- 513 34. Li Jih-Heng and Lin Lih-Fang .Genetic toxicology of abused drugs: a brief review.
514 *Mutagenesb* vol.13 no.6 pp.557-565, 1998
- 515 35. Zhang YT, Zheng QS, Pan J, Zheng RL. Oxidative damage of biomolecules in mouse
516 liver induced by morphine and protected by antioxidants. *Basic Clin Pharmacol*
517 *Toxicol*. 2004; 95:53-8.
- 518 36. Sharp BM, Keane WF, Suh HJ, Gekker G, Tsukayama D, Peterson PK. Opioid
519 peptides rapidly stimulate superoxide production by human polymorphonuclear
520 leukocytes and macrophages, *Endocrinology*. 1985; 117:793-5.
- 521 37. Slupphaug G, Kavli B, Krokan HE. The interacting pathways for prevention and repair
522 of oxidative DNA damage, *Mutat Res*. 2003; 531:231-51.
- 523 38. Skoulis NP, James RC, Harbison RD, Roberts SM. Depression of hepatic glutathione
524 by opioid analgesic drugs in mice. *Toxicol Appl Pharmacol*. 1989; 99:139-47.

- 525 39. Damian GD, Elizabeth AM, Judith MH, and Ruth R. Drug-Induced Oxidative Stress
526 and Toxicity. J Toxicol. 2012, Article ID 645460, 13 pages. doi:
527 10.1155/2012/645460
- 528 40. Shafer DA , Xie Y. Detection of opiate- enhanced increases in DNA damage, HPRT
529 mutants, and the mutation frequency in human HUT- 78 cells. Environmental and
530 Molecular Mutagenesis. 1994; 23:37-44.
- 531 41. Remya NS, Syama S, Sabareeswaran A, Mohanan PV. Investigation of chronic
532 toxicity of hydroxyapatite nanoparticles administered orally for one year in wistar rats.
533 Materials Science and Engineering: C.2017; 76: 518-527
- 534
535
536
537
538

UNDER PEER REVIEW